

Unidirectional processive action of cellobiohydrolase Cel7A on *Valonia* cellulose microcrystals

Tomoya Imai^a, Claire Boisset^{1,a}, Masahiro Samejima^b, Kiyohiko Igarashi^b, Junji Sugiyama^{a,*}

^aWood Research Institute, Kyoto University, Uji, Kyoto 611-0011, Japan

^bGraduate School of Agricultural and Life Science, The University of Tokyo, Bunkyo-ku, Tokyo 113-8256, Japan

Received 22 June 1998; revised version received 7 July 1998

Abstract On the basis of the 'parallel-up' structure of the cellulose crystal, a crystallographic approach to study the mode of action of cellobiohydrolase Cel7A on *Valonia* cellulose microcrystal has been carried out. After incubation with Cel7A, most of the initially smooth and well defined *Valonia* microcrystals displayed fibrillation. However, as the hydrolysis reaction was rather heterogeneous, some microcrystals remained superficially intact. Close investigation on such crystals revealed polar morphology: one end was narrowed extremely or pointed. Electron microdiffraction analysis of these crystals evidenced that the narrowing of the microcrystals occurs at their reducing end side. This was also confirmed by the visualization of selective reducing end labeling at the pointed ends of microcrystals. These lines of investigation are the first demonstration that the processivity of Cel7A action against insoluble highly crystalline celluloses is unambiguously toward non-reducing ends from reducing ends.

© 1998 Federation of European Biochemical Societies.

Key words: Cellobiohydrolase Cel7A; Electron microdiffraction; Reducing end; *Valonia* cellulose; *Trichoderma viride*

1. Introduction

The cellobiohydrolases Cel7A and Cel6A [1] (previously CBHI and CBHII, respectively) are major cellulases produced by *Trichoderma* sp. and are responsible for crystalline cellulose degradation. Traditionally, they have been thought to liberate cellobiose moieties from the non-reducing ends of cellulose chains [2]. However, recent biochemical analyses using soluble oligosaccharide model compounds labeled at one end with ³H [3,4] or ¹⁸O [5] demonstrated that Cel7A attacked at the reducing ends while Cel6A acted from the non-reducing ends of the corresponding oligosaccharides. Both enzymes are now thought to be processive enzymes [6–8], catalyzing cleavage of several consecutive bonds without dissociating from the substrate. Their 3-D structures in complex with various substrate analogues and ligands also demonstrated confirmatively the above mentioned directional binding of the substrate [6,9].

Regarding the insoluble crystalline substrate, i.e. native cellulose microfibril, the directionality of degradation has been less studied. Only electron microscopic investigation of Cel6A degradation on highly crystalline *Valonia* cellulose microcrystals [10] proved a unidirectional mode of action, showing the formation of a pointed tip at the non-reducing end of a micro-

crystal. The result was confirmed when the reducing end staining technique [11] was applied to analyze the pointed microcrystals, where the silver labeling was only found opposite to the pointed end [12].

Degradation by Cel7A on the same *Valonia* microcrystals yielded narrower and subfibrillated crystalline elements [13], but no clear sign was found to indicate its directional mode of action. In this study, however, we have found an experimental condition to yield polar microcrystals, from which we can deduce the directionality of Cel7A action on crystalline substrate. On the basis of the 'parallel-up' packing of cellulose crystals, we have established a method to determine the directionality of cellulose chains in a given microfibril by simple crystallographic consideration [12]. Applying this technique to the pointed microcrystals after hydrolysis, the mode of action of Cel7A on crystalline substrate was analyzed with special attention to the molecular directionality.

2. Materials and methods

2.1. Preparation of microcrystalline suspension of *Valonia*

The vesicles of *Valonia ventricosa* were purified by conventional acid-alkali treatments. The samples were first washed in successive baths of 2% NaOH at room temperature. After neutralization, they were treated in 0.5% HCl for 30 min, followed by boiling in 2% NaOH for 6 h under reflux and solvent exchange every after 2 h. Purified cell walls were cut into small pieces and mechanically disintegrated by homogenization for 10 min at 10000 rpm. They were then hydrolyzed for 5 h in boiling 3.5 N HCl under reflux and continuous strong stirring. The resultant microcrystalline suspension was neutralized by several centrifugal washes with distilled water until achieving neutrality and stored at 4°C in distilled water containing 0.01% NaN₃.

2.2. Enzymatic degradation by CBH Cel7A

The cellobiohydrolase Cel7A (CBHI) was purified from Meicelase, a *Trichoderma viride* cellulase mixture (Meiji-Seika, Tokyo, Japan) according to our previous paper [14]. The hydrolysis was carried out as follows: 8 ml of a 0.5 mg/ml of cellulose suspension was incubated at 40°C in 0.1 M sodium acetate buffer (pH 4.2), containing 1.44 mg of Cel7A. 144 µg of β-D-glucosidase from almonds (EC 3.2.1.21, Sigma) was also added to the reaction in order to avoid the inhibition of Cel7A by the cellobiose produced during hydrolysis. The reaction solution was centrifuged and stopped by washing with 0.2% NaOH. The resulting degraded microcrystals were washed thoroughly by several centrifugations with distilled water and stored at 4°C.

2.3. Silver labeling of reducing ends

Cel7A degraded *Valonia* cellulose microcrystals were stained by the protocol of Kuga and Brown [11]. The suspension of cellulose microcrystals (1 ml) was mixed with 5 ml of 1% thiosemicarbazide (TSC) in aqueous 5% acetic acid. After static incubation at 65°C for 90 min, the suspension was washed by centrifugation. The sample was resuspended in 1 ml of water and mixed with 5 ml of 2% sodium borate with 1% silver proteinate (SP) (Merck). This mixture was kept in the dark at room temperature for 1 h and washed by centrifugation. The final enhancement of the electron density of the TSC-SP treated reducing ends was done by mixing 1 ml of sample with 5 ml of silver

*Corresponding author. Fax: (81) (774) 38-3635.

E-mail: junjis@kuwri.kyoto-u.ac.jp

¹Present address: CERMAV-CNRS, P.O. Box 53, 38041 Grenoble Cedex 9, France.

ammonia solution in a nitric acid-cleaned glass vial for 6–9 min at 95°C until the sample turned brownish. The silver ammonia solution was prepared by adding ammonia solution to a 13.3% silver nitrate solution until the initial brownish color became clear.

2.4. Electron microscopy

All the micrographs and diffraction diagrams were taken with a JEOL-2000EXII operated at 100 kV and recorded on Mitsubishi MEM films. Diffraction contrast imaging in the bright field mode was used to visualize the sample without further contrast enhancement. The images were taken at 1000–6000 \times under low dose exposure with the use of the Minimum Dose System (MDS, Jeol).

The diffraction diagrams were obtained by microdiffraction mode. A small condenser aperture of 20 μ m was inserted and the first condenser lens was fully overfocused to achieve an electron probe of approx. 100 nm. The samples were observed at 2500 \times under extremely low dose conditions with the help of an image intensifier (Fiber Optics Coupled TV, Gatan). When a microcrystal was found, it was rotated to align the fiber axis to the tilt axis using the rotation-tilt holder (SRH holder, Jeol). Diffraction patterns were then recorded from the nearest portion of the microcrystal with the precise tilt angles at -40° , 0° , and 40° about microcrystal length.

Throughout this paper, the indexing of the crystallographic planes of cellulose I refers to the crystal model for cellulose I $_{\alpha}$ [15].

3. Results and discussion

Initial *Valonia* microcrystals display a uniform and well-defined microfibrillar shape. The lateral dimensions are ca.

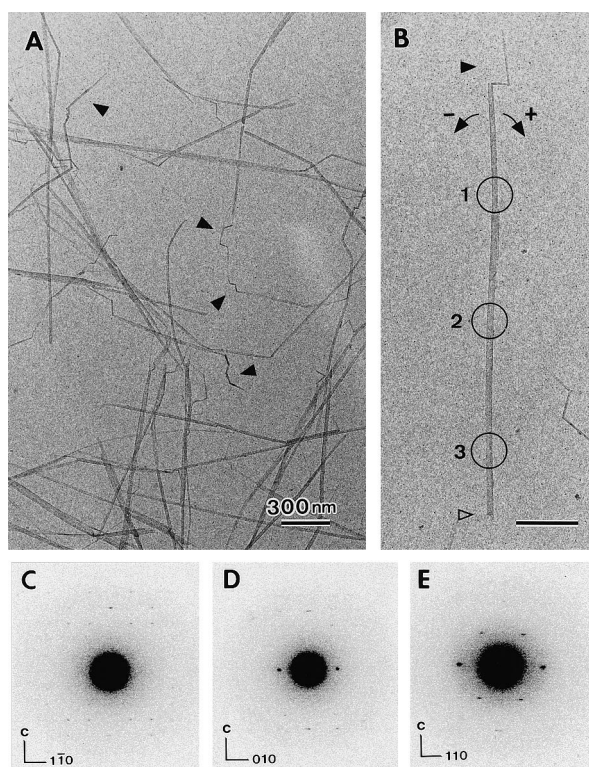


Fig. 1. A bright-field diffraction contrast electron micrograph of *Valonia* cellulose microcrystals after enzymatic degradation for 7 days. Note that only one end of the microcrystals is narrowed and such parts are in most cases kinked by mechanical agitation as indicated by arrowheads (A). Enlarged micrograph of an isolated microcrystal, showing the narrowed end at the top (B). Each circle indicates the position for diffraction diagram. Diagrams C–E are taken from positions 1–3 in B with the corresponding tilt angles of -40° , 0° and 40° . Solid and open arrowheads in B indicate the reducing and non-reducing ends of the crystal respectively. Scale bar 300 nm.

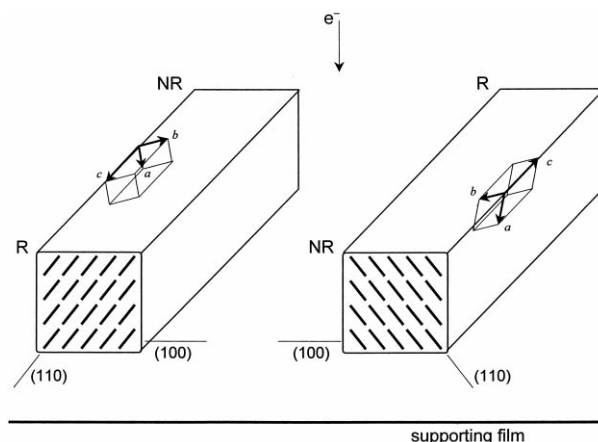


Fig. 2. Theoretical background to determine the molecular polarity of a cellulose microcrystal. Two types of microcrystals having opposite c -axis directionality lie on the film support with their 0.62 nm (100) lattice planes parallel to it. A microcrystal with its c -axis toward the observer (A) gives 0.39 nm (110) diffraction spots after anticlockwise rotation by 40° about the longer axis, while that in B gives the same diagram after clockwise rotation by 40° .

20 \times 20 nm² [16,17] and the lengths are in the range of several hundreds nanometers to a few micrometers. The appearance of the ends of microcrystals is oblique in most cases. This terminal angle is generally higher than 40° with the longer axis of microcrystals.

Most of the initially smooth and well-defined *Valonia* microcrystals displayed fibrillation as reported previously [13]. However, the hydrolysis reaction was rather heterogeneous so that some microcrystals remained superficially intact. The typical appearance of microcrystals after 7 days of incubation with Cel7A is shown in Fig. 1A. Those crystals were as wide as 10–20 nm, but shorter in length than initial crystals. Remarkably, the crystals displayed polar morphology and this phenomenon was most pronounced when the crystals were subjected to mild treatment (without stirring) for longer durations.

The tip of such microcrystals was narrower at one end, and frequently kinked as indicated by arrowheads in Fig. 1A, probably induced by mechanical forces during treatment such as centrifugal washing. This is exemplified in an enlarged micrograph in Fig. 1B, showing small kinked fragments in the upper part of a microcrystal. This observation made us believe that the mode of action of Cel7A was unidirectional.

Chain packing in a cellulose I $_{\alpha}$ unit cell was recently determined such that the reducing ends of cellulose chains pointed the same way to the crystallographic c -axis [12]. This 'parallel-up' packing in cellulose I $_{\alpha}$ crystal allows us to identify the chain polarity in a given crystalline microfibril by analyzing the directionality of the c -axis. The theoretical background is shown schematically in Fig. 2. Since cellulose microcrystals from *Valonia* tend to lie with their (100) 0.62 nm equatorial lattice planes parallel to the specimen support for electron microscopy, two situations can be envisaged, with the c -axis pointing toward (A) or away from (B) the observer. A clear difference between the two settings A and B is the directionality of the (110), 0.39 nm equatorial lattice planes. In order to bring these planes into a Bragg condition, in other words, to orient these planes parallel to the incident electron beams, one has to rotate the microcrystals by -40° and 40° respec-

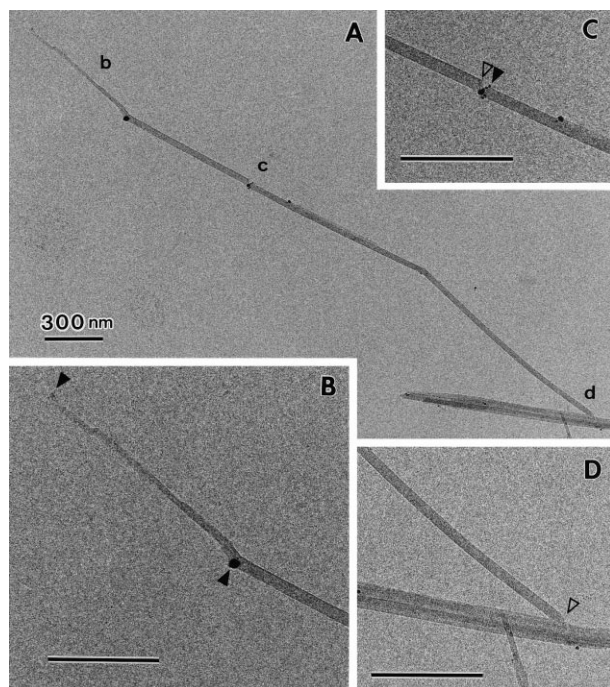


Fig. 3. Electron micrographs of a reducing end silver-stained *Valonia* cellulose microcrystal after enzymatic degradation for 7 days (A). Three areas marked b–d are enlarged in B–D. B: Narrowed end with labeling (solid arrowhead). C: Internal wedge-shaped cut with one side labeled (solid arrowhead) and the other side unlabeled (open arrowhead). D: Unlabeled end (open arrowhead) indicating non-reducing end side. Scale bar 300 nm.

tively about their longer axes in the corresponding settings in A and B. This feature allows us to determine the *c*-axis by obtaining three sets of microdiffraction diagrams from a given microcrystal with precise tilting at -40° , 0° and 40° .

Tilt-microdiffraction analyses for a polar microcrystal as in Fig. 1B were performed, and 15 out of 15 experiments gave identical results as shown in Fig. 1C–E. These diagrams correspond to the situation of Fig. 2B, which implies that the *c*-axis of the microcrystal in Fig. 1B points upward. Accordingly, the reducing end of this microcrystal points upward, and thus the kinked narrowed part is concluded to be the reducing end side of the cellulose microcrystal.

Further confirmation of the above results was provided by the selective reducing end staining technique [11]. Fig. 3A,B shows typical electron micrographs of the resulting microcrystals with one end eroded to a pointed tip and the same end labeled with silver staining. Though not very often, a sharp wedged degradation pattern across the microcrystal width as in Fig. 3C was also observed. The image shows unambiguously that the reducing end staining technique is extremely specific to the reducing end of the chain, and implies that there must have been endo-type degradation during our experiment. Concerning the latter implication, we still need to verify our experimental conditions such as the purity of the Cel7A enzyme we used, and also to scrutinize if such a structure had been created during initial acid hydrolysis to prepare microcrystals or not. However, it is of great interest as it potentially answers the debate as to whether Cel7A is a true exo-processive enzyme that definitely needs chain ends to initiate degradation [18] or a processive enzyme that is capable

of making an initial bite on the crystal as an endo-type enzyme [14,19–21].

Regarding the heterogeneous appearance of the hydrolysates, one may explain this also as a consequence of unidirectional degradation as follows: degradation proceeds from the reducing end of a crystal, creating a fibrillated microcrystal. Since the large active-site tunnel of Cel7A should allow strict binding to the substrate [7], weak agitation may be enough to disintegrate such regions, and thereby narrow fragments would be isolated from the initial microcrystals. At the beginning of treatment, many fibrillated fragments can be seen [13], but after longer duration the reaction leaves non-destroyed portions, polar microcrystals with narrow remains, as observed in this study, because smaller fragments are more susceptible to the hydrolysis.

Comparing the present results with previous data on the mode of degradation by Cel6A from *Trichoderma reesei* [10] and *Humicola insolens* [12], the sharpness of the pointed tips is quite characteristic apart from the directionality of degradation. The origin of this difference must arise from the structure of the enzymes themselves. In fact, both Cel7A and Cel6A are known to have tunnel-shaped active sites but different lengths [6,7]. As discussed by Teeri [2], Cel6A, with a shorter tunnel, might occasionally fall off the substrate and reinitiate hydrolysis at neighboring chain ends, which yields a pointed tip at one end of the crystal. On the other hand, Cel7A, having a longer tunnel, may hold a chain more tightly and keep itself bound to the substrate, which results in fibrillated crystals, i.e. a much longer pointed tip. Thus the observed tip morphology from different enzymes may directly indicate the difference in *processivity* regulated by the 3-D structure of these important enzymes.

Acknowledgements: The study was partly supported by the Joint Research Program between the Japan Society for the Promotion of Science and Centre National de la Recherche Scientifique (J.S.). T.I. was the recipient of a JSPS Fellowship (DC). C.B. was the recipient of a Monbusho Fellowship for foreign young scientists.

References

- [1] Henrissat, B., Teeri, T.T. and Warren, R.A.J. (1998) FEBS Lett. 425, 352–354.
- [2] Teeri, T.T. (1997) Trends Biotechnol. 15, 160–167.
- [3] Versanska, M. and Biely, P. (1992) Carbohydr. Res. 227, 19–27.
- [4] Claeysens, M., van Tilbeurgh, H., Tomme, P. and Wood, T.M. (1989) Biochem. J. 261, 819–825.
- [5] Barr, B.K., Hsieh, Y.-L., Ganem, B. and Wilson, D.B. (1996) Biochemistry 35, 586–592.
- [6] Rouvinen, J., Bergfors, T., Teeri, T., Knowles, J.K.C. and Jones, T.A. (1990) Science 249, 380–386.
- [7] Divne, C., Ståhlberg, J., Reinikainen, T., Ruohonen, L., Pettersson, G., Knowles, J.K.C., Teeri, T.T. and Jones, T.A. (1994) Science 265, 524–528.
- [8] Davies, G. and Henrissat, B. (1995) Structure 3, 853–859.
- [9] Divne, C., Ståhlberg, J., Teeri, T.T. and Jones, T.A. (1998) J. Mol. Biol. 275, 309–325.
- [10] Chanzy, H. and Henrissat, B. (1985) FEBS Lett. 184, 285–288.
- [11] Kuga, S. and Brown Jr., R.M. (1988) Carbohydr. Res. 180, 345–350.
- [12] Koyama, M., Helbert, W., Imai, T., Sugiyama, J. and Henrissat, B. (1997) Proc. Natl. Acad. Sci. USA 94, 9091–9095.
- [13] Chanzy, H., Henrissat, B., Vuong, R. and Schulein, M. (1983) FEBS Lett. 153, 113–117.
- [14] Samejima, M., Sugiyama, J., Igarashi, K. and Eriksson, K.-E.L. (1998) Carbohydr. Res. 305, 281–288.

- [15] Sugiyama, J., Vuong, R. and Chanzy, H. (1991) *Macromolecules* 24, 4168–4175.
- [16] Revol, J.-F. (1982) *Carbohydr. Polym.* 2, 123–134.
- [17] Sugiyama, J., Harada, H., Fujiyoshi, Y. and Uyeda, N. (1985) *Planta* 166, 161–168.
- [18] Srisodsuk, M., Kleman-Leyer, K., Keränen, S., Kirk, T.K. and Teeri, T.T. (1998) *Eur. J. Biochem.* 251, 885–892.
- [19] Amano, Y., Shiroishi, M., Nishizawa, K., Hoshino, E. and Kanda, T. (1996) *J. Biochem.* 120, 1123–1129.
- [20] Armand, S., Drouillard, S., Schülein, S., Henrissat, B. and Driguez, H. (1997) *J. Biol. Chem.* 272, 2709–2713.
- [21] Boisset, C., Armand, S., Drouillard, S., Chanzy, H., Driguez, H. and Henrissat, B. (1998) in: *Carbohydrases from Trichoderma reesei and Other Microorganisms: Structure, Biochemistry, Genetics and Applications* (Claeyssens, M., Ed.), pp. 124–132, The Royal Society of Chemistry, Cambridge.